Available online at www.sciencedirect.com
SCIENCE DIRECT
Journal of Molecular Structure 783 (2006) 122–135
Journal of MOLECULAR STRUCTURE
www.elsevier.com/locate/molstruc

Conformational analysis of the potential anticancer agent ethyl trihydroxycinnamate—A combined raman spectroscopy and ab initio study

J.B. Sousa [a], R. Calheiros [a], V. Rio [b], F. Borges [a,b], M.P.M. Marques [a,c,*]

[a] *Unidade I&D 'Química-Física Molecular', Faculdade de Ciências e Tecnologia, Universidade de Coimbra, 3000 Coimbra, Portugal*
[b] *Departamento de Química Orgânica, Faculdade de Farmácia, Universidade do Porto, 4050-047 Porto, Portugal*
[c] *Departamento de Bioquímica, Faculdade de Ciências e Tecnologia, Universidade de Coimbra, Ap. 3126, 3001-401 Coimbra, Portugal*

Received 13 July 2005; revised 31 August 2005; accepted 6 September 2005
Available online 17 October 2005

Abstract

A conformational analysis of ethyl 3-(3,4,5-trihydroxyphenyl)-2-propenoate (ethyl 3,4,5-trihydroxycinnamate, ETHPPE), a polyphenolic cinnamic ester which displays antiproliferative activity towards human adenocarcinoma cells, was carried out by Raman spectroscopy coupled to ab initio MO calculations. Apart from the optimised geometrical parameters for the most stable conformations of this compound (both for the *trans* and *cis* isomers), the corresponding harmonic vibrational frequencies were obtained. Eighteen distinct geometries were found, 12 for the lowest energy *trans* isomer and six for the *cis* species. The conformational preferences of this system were verified to be mainly ruled by the stabilising effect of π-electron delocalisation, a planar geometry being favoured. The orientation of the ester moiety showed to be the most determinant factor for the overall stability of the molecule. In the light of these results, a complete assignment of the corresponding Raman pattern was performed.

Keywords: Ethyl trihydroxycinnamate; Raman spectroscopy; Ab initio calculations; Conformational analysis

1. Introduction

Phenolic acid derivatives are a group of compounds, present in the human diet in significative amounts, which display an enormous variety of biological functions [1–13], such as antioxidant activity, anti-inflammatory action, and carcinogenesis modulation (e.g. due to their prooxidant capacity that may induce oxidative damage of DNA, proteins or cell lipids). Epidemiological studies linking the prevalence of certain diseases to dietary patterns often show an inverse correlation between a specific diet (particularly rich in leafy green vegetables) and certain pathologic states, namely neoplastic disorders [14,15]. The cytotoxic activity of phenolic systems, closely related to their antioxidant properties [3,16–18], is ruled by their structural characteristics (which determine their lipophilicity and degree of incorporation into the cells). The nature of the biological target, the environmental conditions and the phenol dosage and bioavailability are also factors influencing the therapeutic ability of this kind of compounds.

The evaluation of the antioxidant/antiproliferative activity of phenolic derivatives, either of natural or synthetic origin, aiming at the development of new and more effective anticancer drugs, is nowadays an important area of research in the field of Medicinal Sciences. Indeed, numerous studies have been carried out in order to find new leader compounds (e.g. structurally based on benzoic and cinnamic acids [19,20]), suitable for obtaining either cancer chemopreventive or chemotherapeutic agents. Even though there is a wealth of data on the relevance of phenolic compounds as growth-inhibition agents, the correlation between anticancer activity and chemical structure is far from clear. In fact, no thorough structure-activity relationships (SAR's) may be drawn from the literature, as no systematic study was performed to this date. One of the problems is the scattering of the reported data, which results from different methods of assessment, varying

* Corresponding author. Address: Departamento de Bioquímica, Faculdade de Ciências e Tecnologia, Universidade de Coimbra, Ap. 3126, 3001-401 Coimbra, Portugal. Tel.: +351 239854462; fax: +351 239826541.
E-mail address: pmc@ci.uc.pt (M.P.M. Marques).

0022-2860/$ - see front matter © 2005 Elsevier B.V. All rights reserved.
doi:10.1016/j.molstruc.2005.09.004

substrate systems and miscellaneous concentrations of putative antiproliferative compounds.

The hydroxycinnamic acid derivative *trans*-3-(3,4,5-trihydroxyphenyl)-2-propenoic acid (THPPE) and its esters *trans*-ethyl(3,4,5-trihydroxyphenyl)-2-propenoate (ETHPPE) and diethyl 2-(3,4,5-trihydroxyphenylmethylene)malonate (E2THPPE) (Fig. 1) have lately been synthesised and evaluated for their antioxidant and anticancer activities [21]. The monoester ETHPPE was found to display significant growth-inhibition and cytotoxic effects towards a human cervix adenocarcinoma cell line (HeLa), along with a low toxicity against non-neoplastic cells (human skin fibroblasts), in accordance with reported data for the analogous caffeic and gallic esters [22,23]. Marked structure-activity relationships (SAR's) were found to rule the antioxidant and anticancer activities of these hydroxycinamic acid derivatives. Actually, their biological functions were determined to be intrinsically dependent on the number and relative orientation of the ring hydroxyl substituents, as well as on the presence of alkyl ester side chains and their chemical nature and spatial orientation (e.g. linear vs branched, saturated vs unsaturated). Therefore, the knowledge of these conformational preferences is of the utmost importance for the understanding and/or prediction of the antioxidant and anticancer properties of this kind of systems.

In the present work, a complete conformational analysis was performed for *trans*-ethyl(3,4,5-trihydroxyphenyl)-2-propenoate (ETHPPE), by Raman spectroscopy coupled to ab initio MO calculations (at the DFT level). A comparison with the analogous diester diethyl 2-(3,4,5-trihydroxyphenylmethylene) malonate (E2THPPE) was carried out. This study was intended as a continuation of the one previously reported for the corresponding 3-(3,4,5-trihydroxy-phenyl)-2-propenoic acid (THPPE) [24].

2. Experimental

2.1. Synthesis

Trans-3-(3,4,5-Trihydroxyphenyl)-2-propenoic acid (3,4,5-trihydroxycinnamic acid, THPPE) and *trans*-ethyl 3-(3,4,5-trihydroxyphenyl)-2-propenoate (*trans*-ethyl 3,4,5-trihydroxycinnamate, ETHPPE) were synthesised as described elsewhere [24]. The compounds were identified by both NMR and EI-MS. The data obtained is in accordance with that described in [24].

Diethyl 2-(3,4,5-trihydroxyphenylmethylene)malonate (E2THPPE) was synthesised according to the process described by Hubner et al. [25] with slight modifications. Yield: 70%; IR: 3388, 3282, 1720, 1672, 1600, 1535, 1465, 1375,1326, 1272, 1234, 1149, 1078, 1032, 939, 837, 766, 731, 665, 631. ^{1}H NMR δ: 1.23 (6H, *t*, $COOCH_2C\mathit{H}_3$), 4.19 (2H, *q*, $COOC\mathit{H}_2CH_3$), 4.30 (2H, *q*, $COOC\mathit{H}_2CH_3$), 6.48 (2H, *s*, H(2), H(6)), 7.37 (1H, *s*, H(β)), 9.20 (3H, *s*, OH); ^{13}C NMR δ: *13.8* ($OCH_2\mathit{C}H_3$), *14.1* ($OCH_2\mathit{C}H_3$), *61.1* ($O\mathit{C}H_2CH_3$), *61.3* ($O\mathit{C}H_2CH_3$), *109.4* (*C*H(2, 6)), 121.7 (C(1)), 122.3(C(α), 137.2 (*C*–OH), *142.0* (*C*H(β)), 146.0(*C*-OH), 164.0 (C=O), 166.6 (C=O); EI-MS *m/z* (%): 296 ($M^{+\cdot}$, 100), 251 (36), 222 (38), 205 (49), 178 (38), 150 (58), mp 182–184 °C (156 °C subl.).

Infrared spectra were recorded on a ATI Mattson Genesis Series FTIR spectrophotometer, using potassium bromide disks. Only the most significant absorption bands are reported (ν_{max}, cm^{-1}). ^{1}H and ^{13}C NMR data were acquired at room temperature, on a Brüker AMX 300 spectrometer operating at 300.13 and 75.47 MHz, respectively. DMSO-d_6 was used as a solvent; chemical shifts are expressed in δ (ppm) values relative to tetramethylsilane (TMS) as an internal reference;

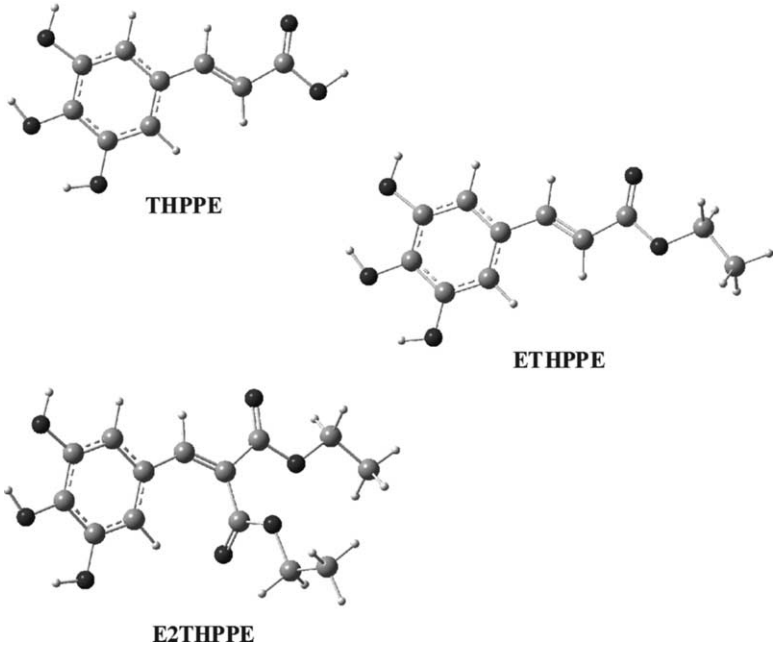

Fig. 1. Representation of the most stable conformers calculated for *trans*-3-(3,4,5-trihydroxyphenyl)-2-propenoic acid (THPPE) and its esters *trans*-ethyl(3,4,5-trihydroxyphenyl)-2-propenoate (ETHPPE) and diethyl 2-(3,4,5-trihydroxy-phenylmethylene)malonate (E2THPPE). (B3LYP/6-31G** level of calculation).

coupling constants (*J*) are given in Hz. Assignments were also made from distortionless enhancement by polarization transfer (DEPT) (underlined values). Electron impact mass spectra (EI-MS) were carried out on a VG AutoSpec instrument; the data are reported as *m/z* (% of relative intensity of the most important fragments). Melting points were obtained on a Köfler microscope (Reichert Thermovar) and are uncorrected.

2.2. Ab initio MO calculations

The ab initio calculations—full geometry optimisation and calculation of the harmonic vibrational frequencies—were performed using the GAUSSIAN 98W program [26], within the Density Functional Theory (DFT) approach, in order to properly account for the electron correlation effects (particularly important in this kind of conjugated systems). The widely employed hybrid method denoted by B3LYP, which includes a mixture of HF and DFT exchange terms and the gradient-corrected correlation functional of Lee, Yang and Parr [27,28], as proposed and parametrised by Becke [29,30], was used, along with the double-zeta split valence basis set 6-31G** [31]. Wavenumbers above 400 cm^{-1} were scaled by a factor of 0.9614 [32] before comparing them with the experimental data. The basis set superposition error (BSSE) correction for the dimerisation energies was estimated by counterpoise (CP) calculations [33], using the MASSAGE option of GAUSSIAN 98W.

Molecular geometries were fully optimised by the Berny algorithm, using redundant internal coordinates [34]: The bond lengths to within ca. 0.1 pm and the bond angles to within ca. 0.1°. The final root-mean-square (rms) gradients were always less than 3×10^{-4} hartree $bohr^{-1}$ or hartree $radian^{-1}$. No geometrical constraints were imposed on the molecules under study.

2.3. Raman spectroscopy

The Raman spectra of the ETHPPE solutions (in Dimethylsulfoxide, DMSO) were obtained at room temperature, in a triple monochromator Jobin-Yvon T64000 Raman system (0.640 m, *f*/7.5) with holographic gratings of 1800 grooves mm^{-1}. The detection system was a non-intensified CCD (Charge Coupled Device) and the entrance slit was set to 200 μm. The 514.5 nm line of an Ar^{+} laser (Coherent, model Innova 300) was used as excitation radiation, providing ca. 50 mW at the sample position. Samples were sealed in Kimax glass capillary tubes of 0.8 mm inner diameter. Under the above mentioned conditions, the error in wavenumbers was estimated to be within 1 cm^{-1}.

Fourier transform Raman spectra were recorded for the solid samples (in order to avoid fluorescence), in a RFS 100/S Bruker spectrometer with a 180° geometry, equipped with an InGaAs detector. Near-infrared excitation was provided by the 1064 nm line of a Nd:YAG laser (Coherent, model Compass-1064/500N). A laser power of 200 mW at the sample position was used in all cases, and resolution was set to 2 cm^{-1}.

2.4. Reagents

Reagents. 3,4,5-trihydroxyaldehyde, *trans*-caffeic acid, dimethylsulfoxide, monoethylmalonate, diethylmalonate and malonic acid were purchased from Sigma-Aldrich Química S.A. (Sintra, Portugal). Dimethylsulfoxide-d_6 (99.8%) was obtained from E. Merck, Darmstadt, Germany. All other

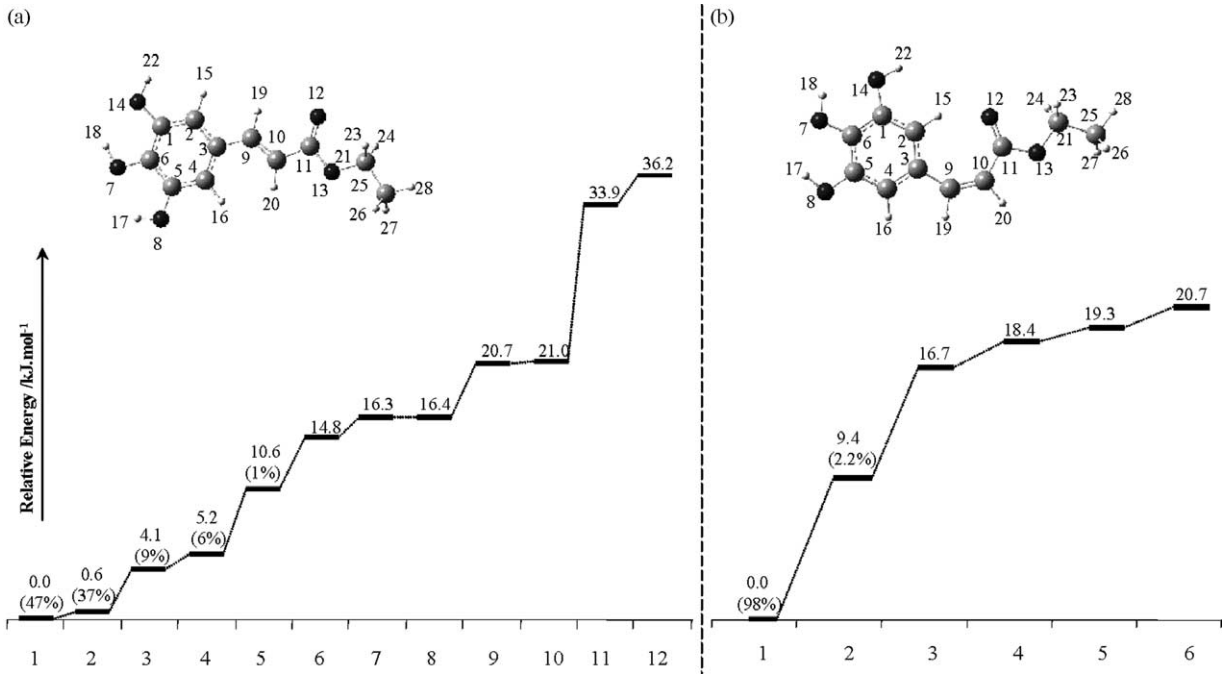

Fig. 2. Schematic representation of the calculated (B3LYP/6-31G**) conformational energies (and populations, at 25 °C) for ethyl 3-(3,4,5-trihydroxyphenyl)-2-propenoate (ETHPPE): (a) *trans* isomer; (b) *cis* isomer. (The atom numbering is included).

reagents and solvents were *pro analysis* grade, purchased from Merck (Lisbon, Portugal).

3. Results and discussion

3.1. Ab initio MO calculations

A complete conformational analysis was carried out for ethyl 3-(3,4,5-trihydroxy-phenyl)-2-propenoate, through ab initio MO calculations: the geometries, relative energies and populations at room temperature were obtained for the distinct possible conformers, for both the *cis* and *trans* ETHPPE isomers (dihedral ($C_{11}C_{10}C_9C_3$) equal to 0° or 180°, respectively, Fig. 2). Harmonic vibrational frequencies were calculated for each structure, in order to confirm the convergence to minima in the potential energy surface. The effect of several structural parameters on the overall stability of the molecule was investigated, namely: (i) orientation of the whole (C_9=C_{10}—ethyl ester) substituent relative to the aromatic ring—internal rotation around the C_9–C_3 bond (dihedral ($C_{10}C_9C_3C_2$) equal to 0° or 180°); (ii) orientation of the ester moiety relative to the aromatic ring—rotation about the C_{11}–C_{10} bond (dihedral ($O_{13}C_{11}C_{10}C_9$) equal to 0° or 180°); (iii) orientation of the ethyl group relative to the carbonyl—rotation around O_{13}–C_{11} (dihedral ($C_{21}O_{13}C_{11}C_{10}$) equal to 180° or 0°, defining a S-*cis* or a S-*trans* conformation,

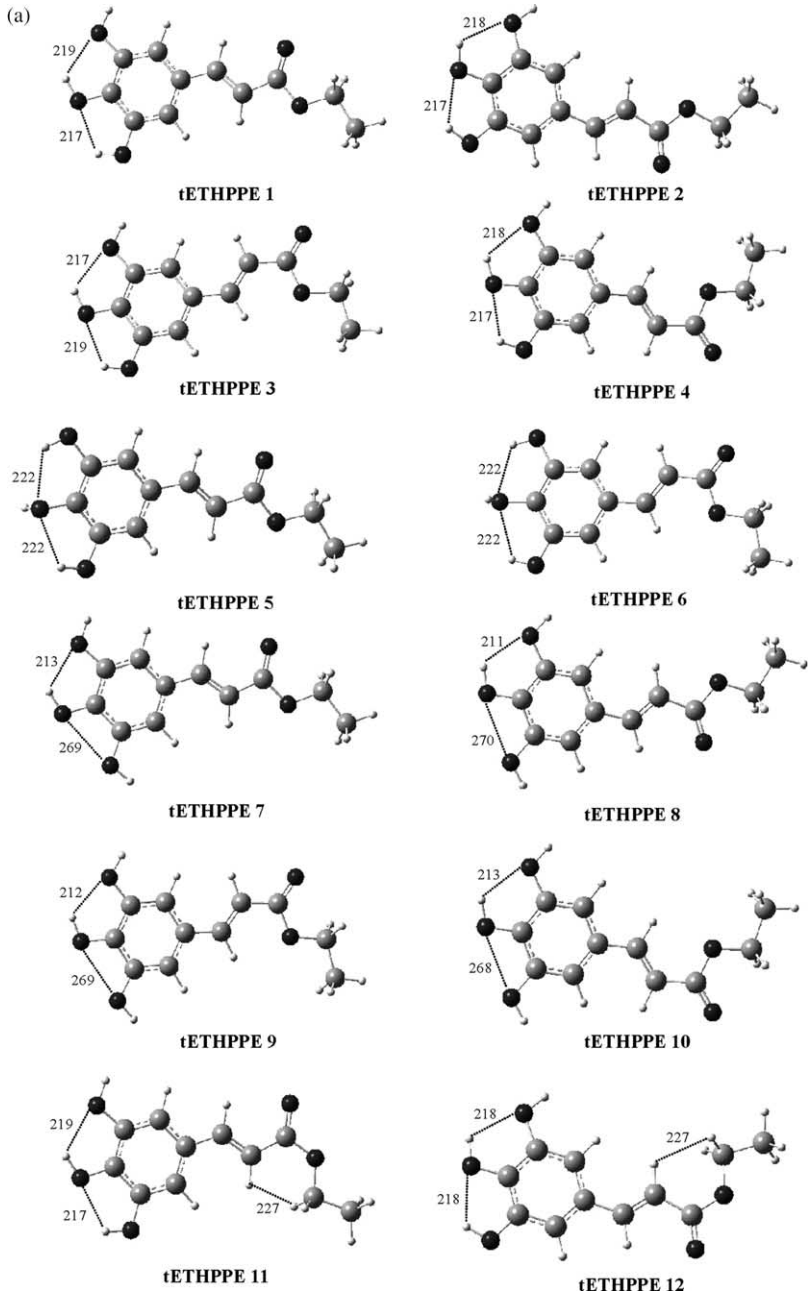

Fig. 3. Representation of the several conformers calculated for ethyl 3-(3,4,5-trihydroxyphenyl)-2-propenoate (ETHPPE)—displaying (C)H···O and (O)H···O intramolecular interactions. (a) *trans* isomer; (b) *cis* isomer. (B3LYP/6-31G** level of calculation. Distances are represented in pm).

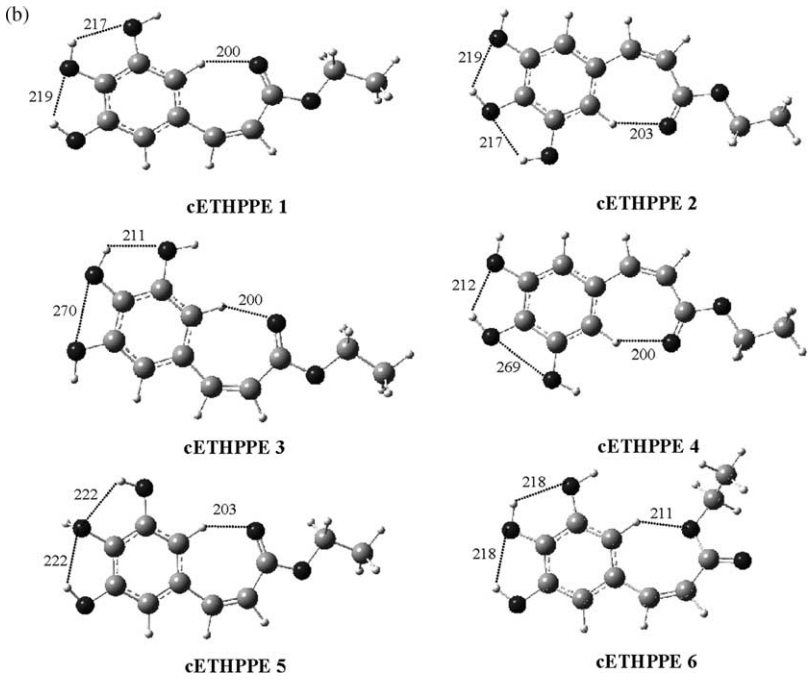

Fig. 3 (*continued*)

respectively); (iv) conformation of the ethyl group—rotation around the O_{13}–C_{21} bond; (v) orientation of the phenolic groups relative to the plane of the ring—either in-plane ($(H_{22}O_{14}C_1C_2)$, $(H_{18}O_7C_6C_1)$ and $(H_{17}O_8C_5C_6)$ equal to 0° or 180°) or out-of-plane. Eighteen different conformers were found for ETHPPE, 12 for the *trans* isomer (tETHPPE) and six for the *cis* species (cETHPPE) (Figs. 2 and 3). A planar geometry showed to be favoured due to the stabilising effect of the π-electron delocalisation between the aromatic ring and the $C_9{=}C_{10}$ and $C_{11}{=}O_{12}$ double bonds, which is maximum when they are coplanar. The only non-planar calculated conformers—tETHPPE 5, tETHPPE 6, cETHPPE 5 and cETHPPE 6—are highly destabilised, tETHPPE 5 being the only one populated at room temperature (1%) (Fig. 2). tETHPPE 5, tETHPPE 6 and cETHPPE 5 display a central hydroxyl group which is almost perpendicular to the plane of the ring—$(H_{18}O_7C_6C_5)$ equal to 91.9°, 91.3° and 94.0°, respectively—while in cETHPPE 6 the ($C_9{=}C_{10}$—ethyl) moiety lies ca. 14.6° out-of-plane ($(C_{10}C_9C_3C_2)$ dihedral) and the ethyl ester is tilted by 83.6° ($(C_{25}C_{21}O_{13}C_{11})$ dihedral).

Similarly to what was verified for THPPE [24], the *cis* isomers of ETHPPE ($(C_{11}C_{10}C_9C_3)$ dihedral equal to 0°)—cETHPPE 1–6 (Figs. 2(b) and 3(b))—display a quite lower stability than the *trans* species ($(C_{11}C_{10}C_9C_3){=}180°$, Figs. 2(a) and 3(a)), despite the possible occurrence of intramolecular medium-strength $H_{15}/H_{16}\cdots O_{12}$ interactions in *cis*-ETHPPE, yielding a seven-membered intramolecular ring ($d(H_{15}/H_{16}\cdots O_{12}$) between 200 and 211 pm). Actually, π-delocalisation is surely more effective in the geometries displaying a linear (zig-zag) $C_9{=}C_{10}$—ethyl ester chain (*trans* geometries). Moreover, the additional stabilisation (by at least 9.4 kJ mol^{-1}) of cETHPPE 1 as compared to cETHPPE 2 is explained by the higher electronic delocalisation in the former, due to the identical orientation of the ring OH's and the C=O group. For these *cis* structures a C_9–C_3 rotation proved to be highly unfavourable: cETHPPE 1 ($(C_{10}C_9C_3C_2){=}0°$, $\Delta E{=}0$) vs cETHPPE 2 ($(C_{10}C_9C_3C_2){=}180°$, $\Delta E{=}9.4$ kJ mol^{-1}), and cETHPPE 3 ($(C_{10}C_9C_3C_2){=}0°$, $\Delta E{=}16.7$ kJ mol^{-1}) vs cETHPPE 4 ($(C_{10}C_9C_3C_2){=}180°$, $\Delta E{=}18.4$ kJ mol^{-1}). Furthermore, an internal rotation around C_{11}–C_{10}—e.g. conversion between conformers cETHPPE 3 and cETHPPE 6 (Fig. 3 (b))—showed to cause a significant degree of steric hindrance involving the ethyl ester moiety, which resulted in an additional rotation of this group relative to the plane of the aromatic ring ($(C_{25}C_{21}O_{13}C_{11}){=}83.6°$ in cETHPPE 6).

Regarding the position of both the ($C_9{=}C_{10}$—ester) moiety and the ethyl ester group relative to the benzene ring—associated to the rotations around C_9–C_3 and C_{11}–C_{10}, respectively—those conformations displaying the same orientation of the carbonyl group and the ring OH substituents (*syn* conformations) showed to be energetically favoured, on account of a more effective π-electron delocalisation: tETHPPE 1 ($(C_{10}C_9C_3C_2){=}180°$, $\Delta E{=}0$) vs tETHPPE 2 ($(C_{10}C_9C_3C_2){=}0°$, $\Delta E{=}0.6$ kJ mol^{-1}), and tETHPPE 3 ($(C_{10}C_9C_3C_2){=}0°$, $\Delta E{=}4.1$ kJ mol^{-1}) vs tETHPPE 4 ($(C_{10}C_9C_3C_2){=}180°$, $\Delta E{=}5.2$ kJ mol^{-1}). For $(C_{10}C_9C_3C_2){=}0°$, in turn, the geometries displaying a close-to-linear arrangement of the ester substituent were found to be stabilised: tETHPPE 2 ($(O_{13}C_{11}C_{10}C_{92}){=}180°$, $\Delta E{=}0.6$ kJ mol^{-1}) vs tETHPPE 3 ($(O_{13}C_{11}C_{10}C_9){=}0°$, $\Delta E{=}4.1$ kJ mol^{-1}) (Figs. 2(a) and 3(a)). Similarly, for $(C_{10}C_9C_3C_2){=}180°$, conformer tETHPPE 1 ($(O_{13}C_{11}C_{10}C_9){=}180°$, $\Delta E{=}0$) is favoured relative to tETHPPE 4 ($(O_{13}C_{11}C_{10}C_9){=}0°$, $\Delta E{=}5.2$ kJ mol^{-1}). This is in agreement with the results previously obtained for THPPE [24]. However, for those

Table 1
Relative energies and calculated (B3LYP/6-31G**) optimised geometries for the most stable conformers of ethyl 3-(3,4,5-trihydroxyphenyl)-2-propenoate (ETHPPE)

ΔE (kJmol^{-1})/μ (D)[a]	tETHPPE 1	cETHPPE 1	tTHPPE[b]	CA[c]
	0; 2.6[d]	0; 1.9	0; 3.5	0; 3.5
Bond lengths (pm)				
C_1–C_6[e]	139.6	140.0	139.6	139.2
C_2–C_1	139.0	138.7	139.0	139.3
C_3–C_2	140.8	141.0	140.9	140.5
C_3–C_9	146.0	146.0	145.9	145.6
C_4–C_3	140.6	141.1	140.7	141.3
C_5–C_4	139.0	139.1	139.0	138.3
C_6–C_5	139.5	139.9	140.2	141.2
C_9–C_{10}	134.6	135.7	134.7	134.8
C_{10}–C_{11}	147.5	147.1	147.2	147.0
C_{21}–C_{25}	151.7	151.7	–	–
C_1–O_{14}	137.5	137.6	137.5	–
C_5–O_8	136.8	136.3	136.1	137.5
C_6–O_7	136.8	136.7	136.8	135.6
C_{11}–O_{12}	121.8	122.2	121.8	121.8
C_{11}–O_{13}	135.7	135.9	136.1	136.2
C_{21}–O_{13}	144.0	144.2	–	–
O_{14}–H_{22}	96.5	96.6	96.5	–
O_7–H_{18}	96.9	96.9	96.9	97.0
O_8–H_{17}	96.9	96.9	96.9	97.0
O_{13}–H_{21}	–	–	97.2	97.2
C_1–H_{14}	–	–	–	108.5
C_2–H_{15}	108.7	108.4	108.7	108.6
C_4–H_{16}	108.3	108.5	108.3	108.7
C_9–H_{19}	108.9	109.0	108.9	108.9
C_{10}–H_{20}	108.5	108.5	108.4	108.5
C_{21}–H_{23}	109.5	109.5	–	–
C_{21}–H_{24}	109.5	109.5	–	–
C_{25}–H_{26}	109.4	109.4	–	–
C_{25}–H_{27}	109.4	109.4	–	–
C_{25}–H_{28}	109.4	109.4	–	–
Bond angles (degrees)				
C_2–C_3–C_4	119.2	119.1	119.2	118.1
C_9–C_3–C_2	118.0	122.7	118.0	118.9
C_{10}–C_9–C_3	128.0	128.0	128.0	128.2
C_{11}–C_{10}–C_9	119.9	120.1	119.8	111.5
C_{10}–C_{11}–O_{13}	110.7	110.7	111.5	111.5
C_{21}–O_{13}–C_{11}	115.7	115.6	–	–
C_{25}–C_{21}–O_{13}	107.5	107.5	–	–
O_{14}–C_1–C_2	125.0	124.9	125.0	–
O_7–C_6–C_1	122.4	122.2	122.4	120.3
O_8–C_5–C_6	119.9	120.1	119.9	114.4
O_{12}–C_{11}–O_{13}	123.2	123.2	122.0	121.9
C_5–O_8–H_{17}	107.8	107.8	107.9	110.1
C_6–O_7–H_{18}	108.0	108.0	108.0	107.8
C_1–O_{14}–H_{22}	109.8	109.8	109.9	–
C_{11}–O_{13}–H_{21}	–	–	105.6	105.5
O_{13}–C_{21}–H_{23}	108.9	108.9	–	–
C_{21}–C_{25}–H_{26}	110.9	110.9	–	–
C_{21}–C_{25}–H_{27}	109.9	109.9	–	–
C_3–C_9–H_{19}	116.0	116.1	115.9	116.0
C_9–C_{10}–H_{20}	123.2	123.3	123.3	123.3
dihedral angles (degrees)				
C_3–C_4–C_5–C_6	0.0	0.0	0.0	0.0
C_9–C_3–C_4–C_5	180.0	180.0	−180.0	180.0
C_{10}–C_9–C_3–C_2	180.0	0.0	−180.0	180.0
C_{11}–C_{10}–C_9–C_3	180.0	180.0	180.0	180.0
O_{12}–C_{11}–C_{10}–C_9	0.0	0.0	0.0	0.0
O_{13}–C_{11}–C_{10}–C_9	180.0	−180.0	−180.0	180.0

(*continued on next page*)

Table 1 (*continued*)

ΔE (kJmol^{-1})/μ (D)[a]	tETHPPE 1	cETHPPE 1	tTHPPE[b]	CA[c]
	0; 2.6[d]	0; 1.9	0; 3.5	0; 3.5
C_{25}–C_{21}–O_{13}–C_{11}	180.0	−180.0	–	–
O_{12}–C_{11}–O_{13}–C_{21}	0.0	0.0	–	–
C_{21}–O_{13}–C_{11}–C_{10}	180.0	−180.0	–	–
H_{15}–C_2–C_3–C_9	0.0	0.0	0.0	0.0
H_{16}–C_4–C_3–C_2	180.0	−180.0	180.0	180.0
H_{18}–O_7–C_6–C_1	0.0	0.0	0.0	180.0
H_{20}–C_{10}–C_9–C_3	0.0	0.00	0.0	0.0
H_{21}–O_{13}–C_{11}–C_{10}	–	–	180.0	180.0
H_{22}–O_{14}–C_1–C_2	0.0	0.0	0.0	–
H_{23}–C_{21}–O_{13}–C_{11}	58.4	58.4	–	–
H_{26}–C_{25}–C_{21}–O_{13}	−60.2	−60.2	–	–
H_{28}–C_{25}–C_{21}–O_{13}	180.0	180.0	–	–

Values for *trans*-THPPE and caffeic acid are included for comparison.

[a] Total dipole moment $1D = 1/3 \times 10^{-2}$ Cm.

[b] Most stable conformer [24].

[c] Most stable conformer [37].

[d] Total value of energy for the most stable conformer of ETHPPE is −802.531196500 (in Hartree, 1 Hartree = 2625.5001 kJ mol^{-1}).

[e] Atoms are numbered according to Fig. 2.

species displaying different orientations of the ring OH's, the effect of the rotation around C_9–C_3 on the conformational energy is almost negligible: for the *trans* species, tETHPPE 7 (($H_{17}O_8C_5C_6$) = 180°, ($C_{10}C_9C_3C_2$) = 180°, ΔE = 16.3 kJ mol^{-1}) vs tETHPPE 8 (($H_{17}O_8C_5C_6$) = 180°, ($C_{10}C_9C_3C_2$) = 0°, ΔE = 16.4 kJ mol^{-1}); for the *cis* isomer, cETHPPE 3 (($H_{17}O_8C_5C_6$) = 180°, ($C_{10}C_9C_3C_2$) = 0°, ΔE = 16.7 kJ mol^{-1}) vs cETHPPE 4 (($H_{17}O_8C_5C_6$) = 180°, ($C_{10}C_9C_3C_2$) = 180°, ΔE = 18.4 kJ mol^{-1}). Rotation about C_{11}–C_{10}, in turn, has a significant effect: tETHPPE 8 (($H_{17}O_8C_5C_6$) = 180°, ($O_{13}C_{11}C_{10}C_9$) = 180°, ΔE = 16.4 kJ mol^{-1}) vs tETHPPE 9 (($H_{17}O_8C_5C_6$) = 0°, ($O_{13}C_{11}C_{10}C_9$) = 0°, ΔE = 20.7 kJ mol^{-1}).

Internal rotation around O_{13}–C_{11}—defining the relative position of the ester moiety—was found to be the most determinant factor for the overall stability of this kind of systems. Actually, the only two conformers with an ethyl S-*trans* orientation were determined to be greatly unfavoured as compared to their S-*cis* counterparts: tETHPPE 11 (($C_{10}C_9C_3C_2$) = 0°, ΔE = 33.9 kJ mol^{-1}) vs tETHPPE 1 (($C_{21}O_{13}C_{11}C_{10}$) = 180°, ΔE = 0), and tETHPPE 12 (($C_{10}C_9C_3C_2$) = 0°, ΔE = 36.2 kJ mol^{-1}) vs tETHPPE 2 (($C_{21}O_{13}C_{11}C_{10}$) = 180°, ΔE = 0.6 kJ mol^{-1}) (Figs. 2(a) and 3(a)). These S-*trans* geometries are the highest energy ones obtained for ETHPPE, probably as a result of destabilising $H_{20}\cdots H_{26}$ and $H_{20}\cdots H_{27}$ repulsive interactions ($H_{20}\cdots H_{26}/H_{27}$ distances equal to 227 pm) (Fig. 3(a)). In fact, even the non-planar *cis* isomer cETHPPE 6, displaying an S-*cis* ester group, is favoured relative to the *trans* conformers tETHPPE 11 and tETHPPE 12 (ΔE = 20.7 vs 33.9 kJ mol^{-1} and 36.2 kJ mol^{-1}, respectively, Fig. 2), possibly due to the formation of a stabilising intramolecular $H_{15}\cdots O_{13}$ close contact (d($H_{15}\cdots O_{13}$) = 211 pm, Fig. 3) which is not possible in tETHPPE 11 and tETHPPE 12.

Regarding the orientation of the ring hydroxyl groups, it was verified that an identical conformation of the three OH's, coplanar with the ring, rendered the most stable conformers, since it leads to a minimisation of the steric repulsions between adjacent OH's and allows the formation of medium strength intramolecular O··· H bonds (O··· H distances between 217 and 219 pm, Fig. 3). In turn, those geometries where one of these hydroxyls has an opposite orientation relative to the other two, although still in-plane with the aromatic ring (($H_{17}O_8C_5C_6$) = 180°)—tETHPPE 7, tETHPPE 8, tETHPPE 9, tETHPPE 10, cETHPPE 3 and cETHPPE 4—showed to be energetically unfavoured as compared to their counterparts with ($H_{17}O_8C_5C_6$) = 0° (Figs. 2 and 3): for the *trans* isomers—tETHPPE 1 (ΔE = 0) vs tETHPPE 7 (ΔE = 16.3 kJ mol^{-1}), tETHPPE 2 (ΔE = 0.6 kJ mol^{-1}) vs tETHPPE 8 (ΔE = 16.4 kJ mol^{-1}), tETHPPE 3 (ΔE = 4.1 kJ mol^{-1}) vs tETHPPE 9 (ΔE = 20.7 kJ mol^{-1}), and tETHPPE 4 (ΔE = 5.2 kJ mol^{-1}) vs tETHPPE 102 (ΔE = 21.0 kJ mol^{-1}); for the *cis* species—cETHPPE 1 (ΔE = 0) vs cETHPPE 3 (ΔE = 16.7 kJ mol^{-1}), and cETHPPE 2 (ΔE = 9.4 kJ mol^{-1}) vs cETHPPE 4 (ΔE = 18.4 kJ mol^{-1}). In addition, the relative orientation of the central OH (as long as it remains in-plane) is practically irrelevant—tETHPPE 7 (ΔE = 16.3 kJ mol^{-1}) vs tETHPPE 8 (ΔE = 16.4 kJ mol^{-1}). In turn, an out-of-plane hydroxyl group, quasi-perpendicular relative to the benzene ring (($H_{18}O_7C_6C_1$) ca. 90°)—tETHPPE 5, tETHPPE 6 and cETHPPE 5—was verified to be responsible for a clear destabilisation (Fig. 2), along with an orientation of the two neighbouring H_{22} and H_{17} atoms towards the central O_7 (d($H_{17}/H_{22}\cdots O_7$) ca. 222 pm, Fig. 3): regarding the *trans* species—tETHPPE 1 (ΔE = 0) vs tETHPPE 5 (($H_{18}O_7C_6C_1$) = 91.9°, ΔE = 10.6 kJ mol^{-1}), and tETHPPE 3 (ΔE = 4.1 kJ mol^{-1}) vs tETHPPE 6 (($H_{18}O_7C_6C_1$) = 91.3°, ΔE = 14.8 kJ mol^{-1}); for the *cis* isomers—cETHPPE 1 (ΔE = 0) vs cETHPPE 5 (($H_{18}O_7C_6C_1$) = 94.0°, ΔE = 19.3 kJ mol^{-1}). As expected, no minimum energy geometries were obtained when any two ring hydroxyls were directed towards each other. This is in accordance with the results previously reported for the corresponding acid THPPE,

Table 2
Experimental (solid state) and calculated (B3LYP/6-31G**) Raman wavenumbers (cm^{-1}) for the most stable conformers of *trans*-ethyl 3-(3,4,5-trihydroxyphenyl)-2-propenoate (ETHPPE) and diethyl 2-(3,4,5-trihydroxyphenylmethylene)malonate (E2THPPE)

Experimental				Calculated[a]			Approximate description[b]
THPPE[c]	ETHPPE	E2THPPE	tTHPPE[d]	tETHPPE 1 (44%)[d]	tETHPPE 2 (37%)[d]	E2THPPE 1 (21%)[d]	
3412	3399	3474	3696 (72;117)	3695 (72;119)	3694 (61;95)	3688 (62;84)	ν ($O^{14}H$)
3395							$2\times\nu$ (C=O)
3363	3369	3426	3648 (140;180)	3646 (145;191)	3646 (132;169)	3642 (118;162)	ν ($O^{7}H$)
3350	3342	3414	3637 (99;100)	3636 (101;103)	3637 (98;107)	3639 (118;139)	ν ($O^{8}H$)
3319			3619 (87;198)				ν ($O^{13}H$)
	3321	3343					$2\times\nu$ (C=O)
3277	3210	3205					$2\times\nu$ (C=C)
3124	3064		3101 (3;55)	3101 (3;47)	3090 (2;65)		ν_s ($C^2H+C^{10}H$)
3080	3033		3089 (4;14)	3086 (5;15)	3082 (11;41)		ν_{as} ($C^2H+C^{10}H$)
3067		3104	3059 (8;71)			3099 (28;41)	ν (C^2H)
						3091 (1;62)	ν (C^4H)
				3056 (9;74)	3065 (4;20)		ν_s (C^4H+C^9H)
	3009			3044 (1;22)	3049 (1;33)		ν_{as} (C^4H+C^9H)
3053		3046	3045 (1;27)			3042 (0;36)	ν (C^9H)
3020							(1375 + 1640) cm^{-1}
	2988			3015 (36;30)	3015 (37;29)	3020 (29;22)	ν_{as} (CH_2) + ν_{as} (CH_3)
						3018 (36;20)	ν_{as} (CH_2) + ν_{as} (CH_3)
	2965	3004		3008 (28;124)	3008 (28;125)	3011 (23;89)	ν_{as} (CH_3)
		2984				3010 (29;126)	ν_{as} (CH_3)
	2951	2977		2979 (11;84)	2980 (10;85)	2986 (8;80)	ν_{as} (CH_2) + ν_{as} (CH_3)
						2986 (8;70)	ν_{as} (CH_2)
	2942	2965		2942 (21;128)	2942 (21;123)	2947 (18;117)	ν_s (CH_2)
		2943					(1608 + 1325 cm^{-1}) FR ν_{as} (CH)
						2946 (18;74)	ν_s (CH_2)
	2931	2934		2937 (21;151)	2936 (21;154)	2939 (17;122)	ν_s (CH_3)
	2925						(1601 + 1359 cm^{-1}) FR ν_{as} (CH_3)
						2938 (18;150)	ν_s (CH_3)
	2898						(1601 + 1281) cm^{-1}
		1717				1727 (112;39)	ν_{iph} (CC=O)
1640	1660		1739 (258;85)	1719 (183;64)	1722 (188;72)		ν (CC=O)
		1676				1712 (23;282)	ν_{oph} (CC=O)
			1634 (218;659)				ν ($C^9C=C^{10}$)
		1645		1634 (198;962)	1632 (223;1049)	1614 (44;42)	ν ($C^9C=C^{10}$) + ν $(CC)_{ring}$
1612	1601	1625	1601 (157;1606)	1602(141;2059)	1605 (69;704)	1602 (123;361)	ν $(CC)_{ring}$ + ν ($C^9C=C^{10}$)
1583		1608	1599 (157; 1606)	1599 (132;22)	1597 (181;1252)	1584 (280;2437)	ν $(CC)_{ring}$
1538	1511	1536	1517 (133;18)	1517 (236;2)	1518 (213;1)	1518 (265;16)	ν $(CC)_{ring}$
	1475	1465		1473 (5;5)	1474 (6;6)	1473 (4;3)	δ (CH_2) (sciss.) + δ_{as} (CH_3)
						1471 (5;1)	δ (CH_2) (sciss.) + δ_{as} (CH_3)
1453	1424		1459 (232;3)	1459 (19;126)	1455 (61;19)		ν $(CC)_{ring}$ + δ (O^8H)
				1454 (3;22)	1454 (20;24)	1455 (1;12)	δ (CH_2) (sciss.) + δ_{as} (CH_3)
						1454 (77;28)	δ (O^8H) + δ_{as} (CH_3)
						1452 (12;27)	δ_{as} (CH_3) + δ (CH_2) (sciss.)
	1386	1403		1443 (5;25)	1443 (5;25)	1443 (4;31)	δ_{as} (CH_3)
		1388				1442 (6;14)	δ_{as} (CH_3)
						1388 (8;16)	δ_s (CH_3) + ω (CH_2) + δ (C^9H)
	1374			1384 (5;9)	1384 (0;15)	1383 (7;6)	δ_s (CH_3) + ω (CH_2)
						1375 (51;10)	δ_s (CH_3) + δ (C^9H)
1374	1358	1368	1375 (22;96)	1366 (7;119)	1372 (58;135)	1366 (117;279)	ν $(CC)_{ring}$ + δ (O^7H) + δ (O^8H) + δ_s (CH_3) + ν (C^1O)
1355			1362 (1;99)	1360 (20;23)	1354 (149;168)		ν $(CC)_{ring}$ + δ (O^7H) + δ (C^9H) + δ_s (CH_3) + ω (CH_2)
		1325				1350 (38;21)	δ (O^7H) + δ_s (CH_3) + ω (CH_2)
	1316			1345 (13;14)	1348 (4;1)	1348 (10;13)	ω (CH_2) + δ_s (CH_3)
						1337 (32;11)	ω (CH_2) + δ_s (CH_3) + δ (O^7H) + δ (O^8H) + δ (C^9H)
	1281		1329 (33;39)	1309 (211;129)	1313 (40;13)		δ (CH) + δ (OH)
1307			1306 (157;2)			1298 (147;17)	δ (OH) + δ (C^9H) + δ_{as} (C^2H+C^4H)
1289			1292 (428;140)	1295 (43;9)	1294 (85;21)		δ_{as} ($C^9H+C^{10}H$) + δ (OH)

(*continued on next page*)

Table 2 (*continued*)

Experimental				Calculated[a]			Approximate description[b]
THPPE[c]	ETHPPE	E2THPPE	tTHPPE[d]	tETHPPE 1 (44%)[d]	tETHPPE 2 (37%)[d]	E2THPPE 1 (21%)[d]	
						1274 (197;7)	δ (O^8H)+δ ($O^{14}H$)+ν (C^6O)+δ (C^9H)+δ (C^2H)
1245			1261 (178;46)				ν (C^6O)+δ_s ($C^9H+C^{10}H$)+δ (C^2H)+δ (OH)
1236	1236		1221 (118;18)	1278 (864;40)	1270 (308;3)		δ_s ($C^9H+C^{10}H$)+δ (C^2H)+δ (OH)
				1248 (47;61)	1254 (538;108)		δ_s ($C^9H+C^{10}H$)+δ ($O^{14}H$)
				1246 (0;17)	1246 (0;17)	1247 (14;19)	t (CH_2)
						1246 (1;12)	t (CH_2)
						1236 (534;62)	δ (C^2H)+ν (CO)+ω (CH_2)+δ (OH)
1204		1271	1212 (17;20)			1222 (878;132)	δ_{as} (C^2H+C^4H)+δ (OH))$_{ring}$+ν (C^5O)
				1212 (96;12)	1214 (70;13)		δ_{as} (C^2H+C^4H)+δ (O^7H)
	1204	1244				1196 (322;88)	δ (C^9H)+δ (C^2H)+δ (OH)+ν (CO)+ω (CH_2)
1151			1177 (84;2)	1178 (144;39)	1172 (67;14)	1174 (190;6)	δ (O^8H)+δ (C^4H)
	1151			1155 (481;122)	1154 (631;182)		δ_s ($C^9H+C^{10}H$)+ν ($C^{11}O$)
		1156				1142 (157;128)	δ_{as} (C^2H+C^4H)+δ ($O^{14}H$)+δ (O^7H)
				1140 (4;2)	1140 (4;2)	1139 (5;2)	r (CH_2)+r (CH_3)
						1138 (3;2)	r (CH_2)+r (CH_3)
1141			1138 (120;5)				δ_s (C^2H+C^4H)+δ_s ($C^9H+C^{10}H$)+δ ($O^{13}H$)
	1122			1133 (164;185)	1134 (63;103)		δ (O^7H) δ (O^8H)+δ (CH)
		1083				1128 (252;153)	δ (C^4H)+δ ($O^{14}H$)+δ (O^7H)+ν (C^3C^9)
			1132 (3;60)	1128 (184;218)	1124 (263;248)		δ (O^7H)+δ ($O^{14}H$)+ν ($C^{11}O$)
			1105 (103;3)				ν ($C^{11}O$)+δ ($O^{13}H$)+δ_s (C^2H+C^4H)+δ ($C^{10}H$)
				1098 (6;12)	1098 (7;13)	1099 (13;9)	r (CH_3)
						1097 (11;8)	r (CH_3)
						1066 (110;3)	r (CH_3)+ν ($C^{10}C^{11}$)+ν (CO)
				1029 (39;7)	1029 (51;6)		ν ($C^{21}O$)
						1020 (51;3)	ν (CC)+ν (CO)
1005			1015 (573;284)			1016 (115;8)	δ (O^7H)+ν (C^1O)+ν (C^5O)
	1004			1014 (195;9)	1014 (143;5)		δ (O^7H)+δ ($O^{14}H$)+ν (C^5O)
						1002 (64;2)	ν (CC)ethyl
992	982		991 (198;9)	990 (23;2)	991 (23;3)		γ_s ($C^9H+C^{10}H$)
972	940	982	974 (6;6)	974 (12;7)	976 (11;8)	974 (14;6)	ν (CC)$_{ring}$
	873	972	935 (16;9)	961 (7;3)	961 (10;4)		ν ($C^{21}C^{25}$)
		940				950 (10;47)	γ (C^9H)
		896		860 (3;16)	860 (4;15)		r (CH_3)+ν ($C^{21}O$)
		881				884 (2;3)	r (CH_3)+ν (CC)
		868				860 (7;17)	r (CH_3)
868			847 (12;13)				γ_{as}($C^9H+C^{10}H$)+γ (CC)$_{chain}$
	855	849		847 (9;16)	847 (3;14)		γ_{as}($C^9H+C^{10}H$)
						845 (7;13)	r (CH_3)+Δ (OCO)
		825				828 (2;2)	γ_{as} (C^2H+C^4H)
810	811	810	819 (12;2)	819 (11;2)	821 (25;3)		γ (C^4H)
						817 (40;0)	γ_s (C^2H+C^4H)
		785				806 (7;2)	γ (C^4H)+δ (CCC)
		740				783 (0;4)	r (CH_2+CH_3)
	761	769		784 (18;34)	784 (4:38)		Δ (CCC)+ν (C^6O)+r (CH_3)+Δ (COC)
			782 (20;19)				ν (CC)$_{ring}$+ν (C^6O)
		720		781 (0;0)	780 (0;0)	782 (1;1)	r (CH_2+CH_3)
			775 (41;1)				γ (C^2H)
						775 (26;0)	r (CH_2+CH_3)+ν (CC)$_{ring}$+ν (C^6O)
	741			774 (33;1)	766 (25;2)	745 (5;0)	γ (C^2H)+r (CH_2)+r (CH_3)
739			721 (24;2)				γ (C^2H)+Δ (CCC)$_{chain}$
671	698	683	678 (2;3)	743 (6;3)	744 (20;4)		Δ (CCC)+Δ (OCO)

Table 2 (*continued*)

Experimental				Calculated[a]			Approximate description[b]
THPPE[c]	ETHPPE	E2THPPE	tTHPPE[d]	tETHPPE 1 (44%)[d]	tETHPPE 2 (37%)[d]	E2THPPE 1 (21%)[d]	
						718 (26;16)	Γ (OCO)
	671			707 (2;0)	707 (3;0)		Γ (CCC)
		670				653 (38;3)	Δ (CCC)
	647	662		636 (0;0)	636 (0;0)	639 (0;1)	Γ $(CCC)_{ring}$
	623			623 (1;8)	625 (58;2)		Δ (CCC)+Δ (CCO)
		622				617 (11;1)	Δ $(CCC)_{ring}$
		601	637 (2;0)			595 (1;22)	Γ $(CCC)_{ring}$
624	594		616 (11;3)	602 (43;5)	601 (2;13)		Δ (CCC)+Δ (CCO)
605	582	575	608 (61;6)	583 (2;1)	581 (2;0)	517 (2;14)	Γ (CCC)+γ ($O^{13}H$)
		554				557 (13;10)	Δ $(CCC)_{ring}$+Γ $(CCC)_{chain}$
589			581 (82;12)				Δ (CCC)+Δ (OCO)
			558 (26;2)				Γ (CCC)+γ ($O^{13}H$)
541			546 (8;0)	548 (0;0)	548 (1;0)	550 (0;0)	Γ $(CCC)_{ring}$
521	541		522 (0;4)	522 (1;4)	520 (0;4)		Δ $(CCC)_{ring}$
484		483	489 (25;6)			490 (11;4)	Δ (CCC)
	501	449		486 (9;6)	486 (11;5)	481 (1;8)	Δ $(CCC)_{ring}$
452	480	435	454 (11;3)	453 (15;6)	453 (1;4)	420 (5;4)	Δ $(CCC)_{chain}$+Δ (CCO)
434	394	421	426 (51;1)	421 (47;1)	420 (50;2)	419 (27;1)	γ (O^8H)+γ (O^7H)
	352	405		388 (24;4)	387 (17;3)	386 (26;8)	Γ (CCC)+Γ (CCO)
380			387 (20;5)				Γ (CCC)
	331	391		379 (11;1)	380 (7;1)	383 (10;3)	Δ (CCO)
		359				376 (72;2)	γ ($O^{14}H$)+γ (O^8H)+γ (O^7H)+Δ (CCO)
352	317	346	357 (104;2)	357 (108;3)	357 (110;3)	371 (54;2)	γ ($O^{14}H$) +γ (O^8H) +γ (O^7H)
		335				316 (10;3)	γ (O^8H) +γ (CC)
						314 (22;3)	γ (O^8H) +γ (CC)
323	304		316 (10;1)	313 (16;1)	314 (10;1)		Δ (C^1OH)+Δ (C^5OH)
290		306	298 (2;0)	298 (0;1)	298 (7;1)	295 (3;2)	Δ (C^6OH)
		285				286 (12;1)	τ (CH_3)
	273			286 (5;1)	285 (10;1)		Γ (CCC)+Γ (CCO)
264			276 (2;4)				Δ (C^1OH)+Δ ($C^{11}OH$)
						278 (2;0)	τ (CH_3)+Γ (CCO)
				275 (0;0)	276 (0;0)		τ (CH_3)
		268	265 (5;0)			262 (20;2)	τ (CH_3)+Γ (CCC)+γ ($O^{14}H$)
	262	261		263 (3;0)	266 (7;0)	258 (23;2)	τ (CH_3)+Γ (CCC)
241	229	244	251 (7;1)	251 (4;1)	250 (2;3)	256 (54;2)	Γ (CCC)+τ (CH_3)+γ ($O^{14}H$)
		226				244 (80;2)	τ (CH_3)+γ ($O^{14}H$)+γ (O^7H)
			213 (0;3)				Δ $(CCC)_{chain}$
	202			209 (0;4)	214 (182;3)		Δ (CCC)+Δ (CCO)
	191		209 (179;5)	208 (184;4)	204 (0;4)		γ ($O^{14}H$)+γ (O^7H)
		188				204 (2;3)	τ (CH_3)+Δ (CCC)
	177	176		189 (0;3)	188 (0;3)	189 (3;1)	τ (CH_3)+Γ (CCC)
179		163	162 (0;1)	158 (0;0)	158 (0;0)	159 (0;1)	Γ (CCO)+Γ (CCC)
						154 (0;0)	Γ (CCC)
	141	139	137 (1;1)	157 (2;1)	158 (2;1)	143 (2;1)	Δ (CCC)+Δ (CCO)
						109 (0;2)	Γ (CCC)+Γ (CCO)
127				94 (1;0)	94 (1;0)	98 (1;1)	Γ (CCC)+Γ (CCO)
			82 (1;0)			82 (0;1)	Skeletal modes
						70 (0;0)	Skeletal modes
		111	68 (0;0)	60 (0;1)	59 (0;1)	61 (0;0)	Skeletal modes
				56 (0;1)	55 (0;1)	56 (0;0)	Skeletal modes
				55 (1;0)	55 (0;0)		Skeletal modes
						35 (0;0)	Skeletal modes
			34 (2;0)	22 (2;1)	21 (0;1)	26 (2;2)	Skeletal modes
						18 (0;4)	Skeletal modes

Values for *trans*-THPPE are included for comparison. δ, in-plane deformation; *t*, twisting; *r*, rocking; ω, wagging; sciss., scissoring; γ, out-of-plane deformation; Δ, in-plane deformation of skeleton atoms; Γ, out-of-plane deformation of skeleton atoms; iph, in-phase; oph, out-of-phase; FR, Fermi Ressonance.

[a] Wavenumbers above 400 cm^{-1} are scaled by a factor of 0.9614 [32]. (IR intensities in km mol^{-1}; Raman scattering activities in Å amu).

[b] Atoms are numbered according to Fig. 2.

[c] [24]; the calculated wavenumbers are the ones obtained for the most stable conformer.

[d] Relative population (at 25 °C).

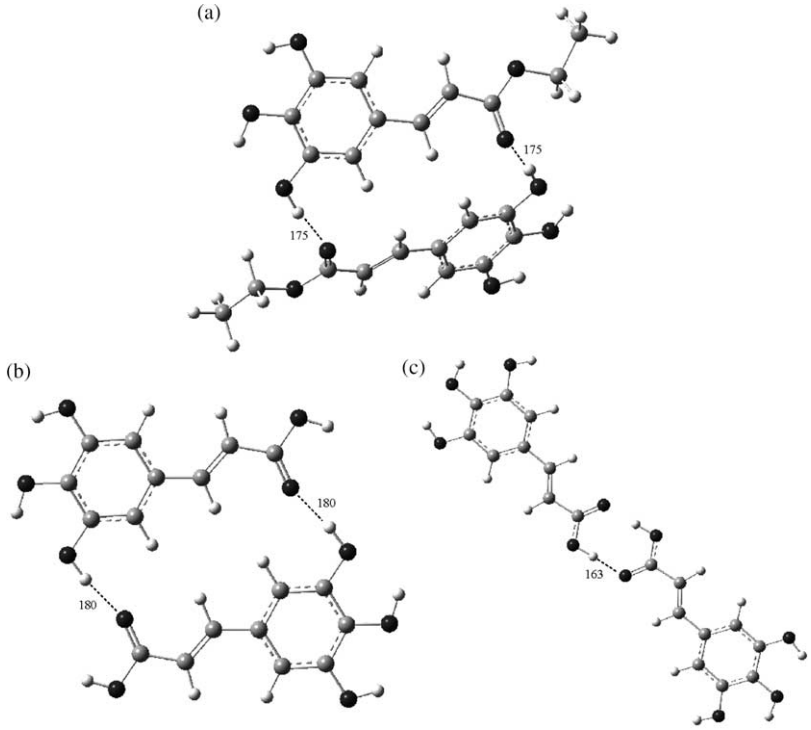

Fig. 4. Representation of calculated dimeric structures for: (a) *trans*-ethyl 3-(3,4,5-trihydroxyphenyl)-2-propenoate (ETHPPE); (b) and (c) *trans*-3-(3,4,5-trihydroxyphenyl)-2-propenoic acid (THPPE). (B3LYP/6-31G** level of calculation. Distances are represented in pm).

for which only one such geometry was calculated as a highly unfavoured conformer [24].

Table 1 comprises the calculated optimised geometries for the lowest energy *trans*- and *cis*-ETHPPE geometries (values for the other conformers are available from the authors upon request). These structural parameters do not deviate much from the X-ray values found in the literature for the analogous dihydroxylated cinnamic acid (known as caffeic acid) [35], and also agree well with the calculated values previously reported for *trans*-caffeic acid [36,37] and *trans*-THPPE [24]. The smaller number of conformers calculated for ETHPPE relative to THPPE (18 vs 21) is a result of destabilising steric hindrances due to the presence of the ethyl ester group, quite bulkier than the carboxylic OH (thus affecting the energy barriers of interconversion between conformers, involving rotation around CO–OR).

The harmonic vibrational frequencies were calculated for all ETHPPE conformers, as well as for the corresponding diester E2THPPE (data available from the authors upon request). Table 2 comprises the calculated wavenumbers for the two most stable ETHPPE geometries, as well as for the lowest energy conformer of E2THPPE, showing a good overall agreement with both the experimental data and the theoretical values obtained by the authors for the analogous acid *trans*-THPPE [24] and for *trans*-caffeic acid [37].

It is well known that this kind of phenolic compounds (either carboxylic acids or esters) occur predominantly as dimeric/oligomeric structures in the condensed phase, formed through intermolecular (O)H···O(=C) interactions. Therefore, calculations were performed for dimeric species of *trans*-ETHPPE and the analogous carboxylic acid *trans*-THPPE, in order to achieve a more accurate representation of these molecules in the solid state. The dimeric structure comprising two equal monomers of tETHPPE 1 (Fig. 4(a)) was found to display quite strong hydrogen close contacts between the carbonyl and the ring hydroxyl substituents—$(O)H_{22}\cdots O_{12}(=C)$ distances of 175 pm—yielding an overall geometry identical to the most stable dimer calculated for THPPE ((O)H···O(=C) equal to 180 pm, Fig. 4(b)). The presence of the ethyl ester groups in the tETHPPE 1 dimer is responsible for a tilted relative orientation of the two monomeric moieties as compared to the planar geometry of the THPPE dimer (Fig. 4(a) and (b)), in order to minimise steric repulsions. This type of close contacts between the ring hydroxyls and the carbonyl group are clearly favoured, even when top-to-top H-bond interations between the terminal carboxylic functions may occur, in the phenolic acid analogues: for THPPE, for instance, the second lowest energy dimeric species was found to correspond to such an interaction (Fig. 4(c)) and displays a conformational energy 4.5 kJ mol^{-1} higher than the most stable dimer (with populations at room temperature equal to 16 and 84%, respectively).

3.2. Raman spectroscopy

A complete assignment of the experimental bands of *trans*-ETHPPE was carried out, based on its calculated vibrational frequencies (Table 2), as well as on experimental and theoretical results previously obtained for analogous compounds, such as caffeic acid [37] and THPPE [24]. The presence of the *cis* isomer is found to be negligible in the product synthesised as presently described, due to its much

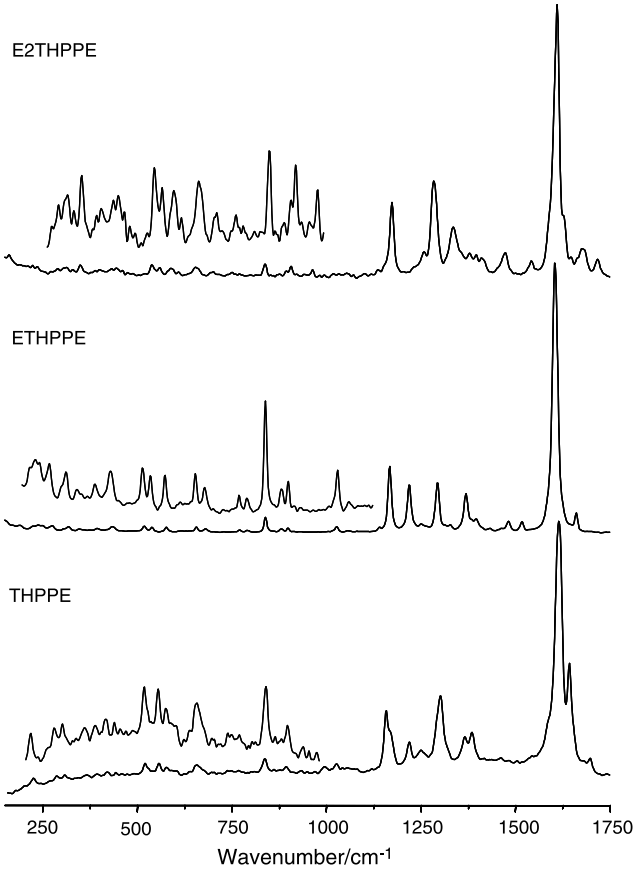

Fig. 5. Experimental Raman spectra (100–1750 cm^{-1}) of *trans*-ethyl 3-(3,4,5-tri-hydroxyphenyl)-2-propenoate (ETHPPE) and the corresponding acid (3-(3,4,5-trihydroxyphenyl)-2-propenoic acid, THPPE) and diethyl ester (diethyl 2-(3,4,5-trihydroxyphenylmethylene)malonate, E2THPPE). (Solid state, 25 °C).

lower stability (which is corroborated by the theoretical results previously discussed).

Fig. 5 comprises the solid state experimental Raman spectra (from 100 to 1750 cm^{-1}) of *trans*-ETHPPE, as well as of the corresponding acid *trans*-THPPE and the diester E2THPPE. The most characteristic features detected for solid ETHPPE were (Fig. 5, Table 2): (i) OH vibrations–stretching modes between ca. 3400 and 3300 cm^{-1}, and deformations from 1360 to 1000 cm^{-1}; (ii) C=O stretching mode (with a rather low Raman scattering activity)—at 1660 cm^{-1} (1640 cm^{-1} in the acid); (iii) C=C stretching vibrations, both from the pendant carbon chain and the aromatic ring, yielding the most intense band in the spectrum (the latter displaying a higher Raman activity)—at ca. 1601 cm^{-1} (at 1612 cm^{-1} in the acid); (iv) CH vibrations–stretching modes, both symmetric and asymmetric, around 3000 and 2900 cm^{-1} respectively, and CH_2/CH_3 deformations, between ca. 1475 and 1100 cm^{-1}; (v) CH_3 torsion, around 260 cm^{-1}.

While for both the acid and the monoester the C=C bonds from the carbon chain and the aromatic ring gave rise to an intense feature at 1612 and 1601 cm^{-1}, respectively, two bands were observed for the diester, at 1608 and 1625 cm^{-1}, assigned to $\nu_{C=C(ring)}$ and ($\nu_{C=C(chain)}+\nu_{C=C(ring)}$) (Fig. 5, Table 2), the former having a much higher calculated Raman activity. Regarding the ester ν_{C-O} oscillator, a deviation to high wavenumbers was observed when going from THPPE (1132/1105 cm^{-1} calculated) to the esters ETHPPE (1204 cm^{-1} experimental vs 1248 cm^{-1} calculated) and E2THPPE (1271/1244 cm^{-1} experimental vs 1236/1222/1196 cm^{-1} calculated) (Table 2), which may be explained by the larger force constant of the C–O bond in the latter, due to the enhancement of the inductive effect upon esterification. As to the $\nu_{C=O}$ vibrational mode, a shift to high frequencies was detected for the esters (Fig. 5): 1640 cm^{-1} for THPPE, 1660 cm^{-1} for ETHPPE, and 1717 and 1676 cm^{-1} for E2THPPE (respectively, in-phase and out-of-phase vibrations). This behaviour was not predicted by the calculations for the isolated molecule—$\nu_{C=O}$ at 1739, 1719 and 1727/1712 for THPPE, ETHPPE and E2THPPE, respectively (Table 2)—since these do not consider the intermolecular close contacts occurring in the condensed phase and mostly affecting the modes involving the carbonyl and hydroxyl groups.

In fact, both the $\nu_{C=O}$ and ν_{OH} oscillators were found to display a significant downward shift relative to the calculated values (Table 2), as expected according to the previous results on caffeic acid [37] and THPPE [24]. This is a consequence of the presence of dimers in the condensed phase, typical of this type of phenolic carboxylic acids/esters, where stabilising (O)H···O(=C) intermolecular close contacts give rise to rather stable dimeric/oligomeric species [38,39] (Fig. 4). These findings are corroborated by the ab initio results obtained for both THPPE [24] and ETHPPE monomeric vs dimeric geometries: for the OH group involved in an intermolecular close contact in ETHPPE ν_{OH} was shown to shift from ca. 3695 to 3430 cm^{-1} (in good agreement with the observed bands at 3399–3342 cm^{-1}, Table 2). These ν_{OH} vibrations usually yield broad Raman features (not easily detected experimentally), as a consequence of these intermolecular hydrogen close-contacts. The ester C=O stretching ($\nu_{C=O}$), also known to be affected by dimerisation, showed an expected deviation to low frequencies upon H-bond formation: from 1719 cm^{-1} in the monomer to 1682/1657 cm^{-1} in the dimeric species (in accordance with the experimental value of 1660 cm^{-1}, Table 2). Furthermore, the bands ascribed to the C_1–O_{14} stretching, and particularly to the in-plane $O_{14}H_{22}$ bending mode, displayed a clear upward shift due to dimer formation: from 1366 and 1248 cm^{-1} (respectively) in the monomer to 1390 and 1440 cm^{-1} in the dimer. Consequently, the calculated wavenumbers associated to the groups prone to be involved in intermolecular hydrogen close-contacts (dimeric structures) presented a very good agreement with the experimental values obtained for the solid.

In view of better understanding the effect of dimerisation on the Raman pattern of ETHPPE, particularly on the $\nu_{C=O}$ oscillator, spectra were obtained for DMSO solutions. DMSO was chosen has a solvent since it is Raman-transparent in the spectral region of interest, and any possible interaction with the ester—via (O)H···O(=S) close contacts, reflected in a band at ca. 1750 cm^{-1} [40]—is known to occur only for very high

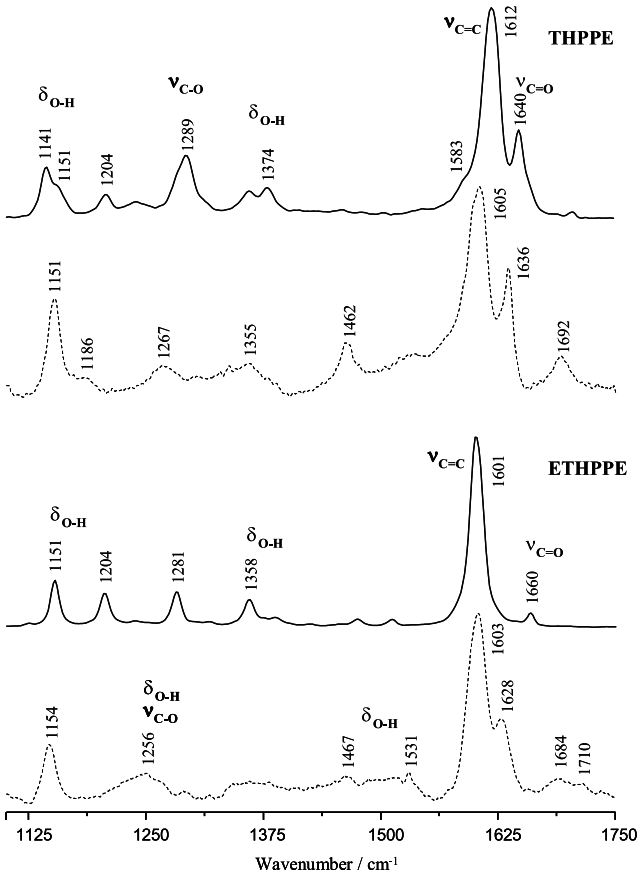

Fig. 6. Experimental Raman spectra (1100–1750 cm^{-1}, at 25 °C) of *trans*-ethyl 3-(3,4,5-trihydroxyphenyl)-2-propenoate (ETHPPE) and the corresponding acid *trans*-3-(3,4,5-trihydroxyphenyl)-2-propenoic acid (THPPE), both in the solid state and in DMSO 40 mM solution. (Solid line—solid state; dotted line—solution).

solvent:solute ratios (much higher than the ones used along this study).

While for the solid the C=O group gave rise to only one stretching band, at 1660 cm^{-1}, for ETHPPE-DMSO 40 mM-solution two features were assigned to $\nu_{C=O}$, at 1710 and 1684 cm^{-1} (Fig. 6), the former being slightly enhanced in the 20 mM-solution. Considering that the dimer:monomer ratio decreases upon dilution, i.e. when going from the solid sample to the solution, these two bands were ascribed to the free and hydrogen-bonded forms of the C=O group, respectively (in analogy with the THPPE system previously studied [24]). In fact, the higher relative population of monomeric species in the solution is reflected in the observation of free carbonyl groups, not involved in intermolecular H-bonds—$\nu_{C=O}$ mode at 1710 cm^{-1} in agreement with the value of 1719 cm^{-1} calculated for the isolated molecule (Table 2). The H-bonded C=O groups give rise to a stretching band at 1684 cm^{-1}, which corresponds to the band at 1660 cm^{-1} detected for the solid. The intensity increase of the 1710 cm^{-1} feature upon dilution corroborates this hypothesis. When compared to the substituted benzaldehydes for which this type of dimeric structures has been initially reported [41,42], the frequency shift observed for ETHPPE (and analogous systems) is quite larger, on account of the higher electronic delocalisation occuring in these hydroxycinnamic derivatives due to the presence of the unsaturated linear carbon chain: ca. 10 cm^{-1} vs ca. 50 cm^{-1}, respectively.

The C–O stretching vibration also showed to be affected by this dimer–monomer equilibrium, displaying a shift from 1281 cm^{-1} in the solid, to 1256 cm^{-1} in the solution (Fig. 6). The typical phenolic OH bending vibration at about 1358 cm^{-1} was also found to suffer changes upon dimerisation (from the solution to the solid state, Fig. 6), which is easily understandable in view of the involvement of some of these hydroxyl groups in the dimerisation process (Fig. 4). The $\nu_{C=C}$ mode from the carbon chain, in turn, undergoes an upward shift when going from the dimer (1601 cm^{-1}) to the monomer (1628 cm^{-1}), while the ring $\nu_{C=C}$ appears at roughly the same frequency (1603 cm^{-1}). Moreover, a new feature is detected in the spectrum of the solution at 1256 cm^{-1} (Fig. 6), which is assigned to both C_1–O_{14} stretching and in-plane C_1–O_{14}–H_{22} deformation—thus being directly affected by the formation of dimeric structures such as the one represented in Fig. 4.

4. Conclusion

The conformational analysis performed for ETHPPE rendered eighteen distinct conformers, twelve for the *trans* isomer and six for the *cis* species, with structural differences concerning the conformation of the ethyl ester group and the adjacent unsaturated carbon chain, as well as the orientation of the three ring hydroxyl substituents. Two of these conformers—tETHPPE 1 ($\Delta E = 0$) and tETHPPE 2 ($\Delta E =$ 0.6 kJ mol^{-1})—were found to be particularly stable, with populations at room temperature of 47 and 37%, respectively. The conformational preferences of this molecule, mainly determined by an effective π-electron delocalisation coupled to a minimisation of repulsive interactions, were found to be: a planar geometry; an S-*cis* orientation of the ester group; a ($C_{11}C_{10}C_9C_3$) dihedral equal to 180°; an identical orientation of the hydroxyl groups, coplanar with the ring; a *syn* conformation of the carbonyl group and the ring OH's. The preference for planarity was expected, since it favours electron delocalisation through the expanded π system of the hyperconjugated molecule of ETHPPE. Thus, non-planar geometries arose only in order to overcome steric hindrance destabilising factors (such as H···H interactions), whose minimisation resulted to be more favourable then the maintenance of planarity.

Comparison of the conformational results presently described with the ones reported for THPPE allows to conclude that the additional degrees of freedom introduced by esterification are mainly reflected in the internal rotation around the O_{13}–C_{11} bond, which showed to be the most important factor determining the overall stability of the ETHPPE molecule. Also, the S-*cis* to S-*trans* energy difference was found to be almost unaffected by the presence of the ethyl ester group as compared to the carboxylic function (ΔE ca. 11.5 kJ mol^{-1} for both ETHPPE and THPPE). Furthermore, the conformational analysis performed for the analogous dihydroxylated cinnamic acid (CA) [37] evidences that

inclusion of a third OH ring substituent (as in THPPE and ETHPPE) does not significantly affect the structural preferences described for this kind of phenolic systems.

A complete assignment of the solid state Raman spectrum of *trans*-ETHPPE was carried out, in the light of the ab initio calculations and the reported data on the analogous compounds THPPE [24] and caffeic acid [37]. A quite good agreement was found between the results now obtained for ETHPPE—both calculated and experimental vibrational wavenumbers—and the data found in the literature for similar molecules, both from theoretical and spectroscopic studies [24,37–39,43,44].

In conclusion, this kind of conformational analysis carried out for phenolic derivatives, through ab initio theoretical calculations coupled to vibrational spectroscopy, are of the utmost importance for understanding the structure-activity relationships (SAR's) ruling the biological activity of such compounds. In fact, the hydroxycinnamic acid derivatives presently studied were found to display both antioxidant [21] and cytotoxic properties against human cancer cell lines [22,23], that can only be accurately interpreted in the light of the corresponding conformational analysis.

Acknowledgements

The authors thank the Chemistry Department of the University of Aveiro, where the FT-Raman experiments were carried out. RC acknowledges financial support from FCT—PhD fellowship SFRH/BD/16520/2004.

References

[1] O.I. Aruoma, A. Murcia, J. Butler, B. Halliwell, J. Agric. Food Chem. 41 (1993) 1880.
[2] T. Nakayama, Cancer Res. 54 (1994) 1991 Suppl..
[3] C.A. Rice-Evans, N.J. Miller, G. Paganga, Free Radic. Biol. Med. 20 (1996) 933.
[4] G. Cao, E. Sofic, L. Prior, Free Radic. Biol. Med. 22 (1997) 749.
[5] B. Halliwell, J.C. Gutteridge, Free Radicals in Biology and Medicine, Oxford Science Publications, 1999.
[6] E. Sergediene, K. Jonsson, H. Szymusiak, B. Tyrakowska, I.M.C.M. Rietjens, N. Cenas, FEBS Lett. 462 (1999) 392.
[7] M. Inoue, N. Sakaguchi, K. Isuzugawa, H. Tani, Y. Ogihara, Biol. Pharm. Bull. 23 (2000) 1153 (and refs. therein).
[8] G. Roy, M. Lombardía, C. Palacios, A. Serrano, C. Cespón, E. Ortega, P. Eiras, S. Lujan, Y. Revilla, P. González-Porqué, Arch. Biochem. Biophys. 383 (2000) 206 (and refs. therein).
[9] T. Gao, Y. Ci, H. Jian, C. An, Vibr. Spectrosc. 24 (2000) 225.
[10] W.Y. Chung, Y.J. Jung, Y.J. Surh, S.S. Lee, K. Park, Mutat. Res. 496 (2001) 199.
[11] A. Russo, R. Longo, A. Vanella, FitoterapiaSuppl. 1(2002) S21.
[12] C. Anselmi, M. Centini, P. Granata, A. Sega, A. Buonocore, A. Bernini, R.M. Facino, J. Agric. Food. Chem. 52 (2004) 6425.
[13] Y.T. Lee, M.J. Don, C.H. Liao, H.W. Chiou, C.F. Chen, L.K. Ho, Clin. Chim. Acta. 352 (2005) 135.
[14] G.J. Kelloff, Adv. Cancer Res. 78 (2000) 199.
[15] N.N. Mahmoud, A.M. Carothers, D. Grunberger, R.T. Bilinski, M.R. Churchill, C. Martucci, H.L. Newmark, M.M. Bertagnolli, Adv. Cancer Res. 21 (2000) 921.
[16] A. Serrano, C. Palacios, G. Roy, C. Cespón, M.L. Villar, M. Nocito, P. González-Porqué, Arch. Biochem. Biophys. 350 (1) (1998) 49.
[17] F. Natella, M. Nardini, M. Di Felice, C. Scaccini, J. Agric. Food Chem. 47 (1999) 1453.
[18] F.A.M. Silva, F. Borges, C. Guimarães, J.L.F.C. Lima, C. Matos, S. Reis, J. Agric. Food Chem. 48 (2000) 2122.
[19] A. Hosoda, Y. Ozaki, A. Kashiwada, M. Mutoh, K. Wakabayashi, E. Nomura, H. Taniguchi, Bioorg. Med. Chem. 10 (2002) 1189.
[20] A.Y.T. Lee, M.J. Don, P.S. Hung, Y.C. Shen, Y.S. Lo, K.W. Chang, C.F. Chen, L.K. Ho, Cancer Lett. 223 (2005) 19.
[21] V. Rio, C. Siquet, S. Reis, M.P.M. Marques, J.B. Sousa, F. Borges, Cancer Lett. submitted.
[22] C.A. Gomes, T. Girão da Cruz, J.L. Andrade, N. Milhazes, F. Borges, M.P.M. Marques, J. Med. Chem. 46 (2003) 5395.
[23] S.M. Fiuza, C. Gomes, L.J. Teixeira, M.T. Girão da Cruz, M.N.D.S. Cordeiro, N. Milhazes, F. Borges, M.P.M. Marques, Bioorg. Med. Chem 12 (2004) 3581.
[24] S.M. Fiuza, E. Van Besien, N. Milhazes, F. Borges, M.P.M. Marques, J. Mol. Struct. 693 (2004) 103.
[25] K. Freudenberg, H.H. Hubner, Chem. Ber. 85 (1952) 1181.
[26] M.J. Frisch, G.W. Trucks, H.B. Schlegel, G.E. Scuseria, M.A. Robb, J.R. Cheeseman, V.G. Zakrzewski, J.A. Montgomery Jr., R.E. Stratmann, J.C. Burant, S. Dapprich, J.M. Millam, A.D. Daniels, K.N. Kudin, M.C. Strain, O. Farkas, J. Tomasi, V. Barone, M. Cossi, R. Cammi, B. Mennucci, C. Pomelli, C. Adamo, S. Clifford, J. Ochterski, G.A. Petersson, P.Y. Ayala, Q. Cui, K. Morokuma, D.K. Malick, A.D. Rabuck, K. Raghavachari, J.B. Foresman, J. Cioslowski, J.V. Ortiz, A.G. Baboul, B.B. Stefanov, G. Liu, A. Liashenko, P. Piskorz, I. Komaromi, R. Gomperts, R.L. Martin, D.J. Fox, T. Keith, M.A. Al-Laham, C.Y. Peng, A. Nanayakkara, M. Challacombe, P.M.W. Gill, B. Johnson, W. Chen, M.W. Wong, J.L. Andres, C. Gonzalez, M. Head-Gordon, E.S. Replogle, J.A. Pople, Gaussian 98, Revision A.9, Gaussian Inc., Pittsburgh PA, USA, 1998.
[27] C. Lee, W. Yang, R.G. Parr, Phys. Rev. B 37 (1988) 785.
[28] B. Miehlich, A. Savin, H. Stoll, H. Preuss, Chem. Phys. Lett. 157 (1989) 200.
[29] A. Becke, Phys. Rev. A 38 (1988) 3098.
[30] A. Becke, J. Chem. Phys. 98 (1993) 5648.
[31] G.A. Petersson, A. Bennett, T.G. Tensfeldt, M.A. Al-Laham, W.A. Shirley, J. Mantzaris, J. Chem. Phys. 89 (1988) 2193.
[32] A.P. Scott, L. Radom, J. Phys. Chem. 100 (1996) 16502.
[33] S.F. Boys, F. Bernardi, Molec. Phys. 19 (1970) 553.
[34] C. Peng, P.Y. Ayala, H.B. Schlegel, J. Frisch, Comput. Chem. 17 (1996) 49.
[35] S. García-Granda, G. Beurskens, P.T. Beurskens, T.S.R. Krishna, G.R. Desiraju, Acta Cryst. C43 (1987) 683.
[36] E. Bakalbassis, A. Chatzopoulou, V.S. Melissas, M. Tsimidou, M. Tsolaki, A. Vafiadis, Lipids 36 (2001) 181.
[37] E. van Besien, M.P.M. Marques, J. Mol. Struct.(THEOCHEM) 625 (2003) 265.
[38] S. Sánchez-Cortés, V. García-Ramos, Spectrochim. Acta A55 (1999) 2935.
[39] S. Sánchez-Cortés, J.V. García-Ramos, Appl. Spec. 54 (2000) 230.
[40] P. Novak, D. Vikic-Topic, Z. Meic, S. Sekusak, A. Sabljic, J. Mol. Struct. 356 (1995) 131.
[41] N. Karger, A.M. Amorim da Costa, P.J.A. Ribeiro-Claro, J. Phys. Chem. A 103 (1999) 8672.
[42] M.P.M. Marques, A.M. Amorim da Costa, P.J.A. Ribeiro-Claro, J. Phys. Chem. A 105 (2001) 5292.
[43] S. Sánchez-Cortés, J.V. García-Ramos, J. Colloid Interface Sci. 231 (2000) 98.
[44] R. Calheiros, N. Milhazes, F. Borges, M.P.M. Marques, J. Mol. Struct. 692 (2004) 91.